NIH Public Access
Author Manuscript
Biochim Biophys Acta. Author manuscript; available in PMC 2012 June 28.

Published in final edited form as:
Biochim Biophys Acta. 2008 December ; 1778(12): 2671–2681. doi:10.1016/j.bbamem.2008.09.011.

Characterization of the glycosylphosphatidylinositol-anchor signal sequence of human Cryptic with a hydrophilic extension

Kazuhide Watanabe[1], **Tadahiro Nagaoka**[1], **Luigi Strizzi**[1,2], **Mario Mancino**[1,3], **Monica Gonzales**[1], **Caterina Bianco**[1], and **David S. Salomon**[1,*]

[1]Tumor Growth Factor Section, Mammary Biology & Tumorigenesis Laboratory, Center for Cancer Research, National Cancer Institute, National Institutes of Health Bethesda, MD

[2]Children's Memorial Research Center, Robert H. Lurie Cancer Center, Northwestern University Feinberg School of Medicine, Chicago, IL

[3]Oncology Research Center of Mercogliano (AV), Italy

SUMMARY

Epidermal Growth Factor-Cripto-1/FRL-1/Cryptic (EGF-CFC) proteins, including human Cripto-1 (hCFC2/hCR-1) and human Cryptic (hCFC1), are membrane-associated Nodal co-receptors, which have critical roles in vertebrate development. Most of the EGF-CFC proteins have been experimentally proven or predicted to be glycosylphosphatidylinositol (GPI)-anchored proteins. However, unlike other EGF-CFC proteins, hCFC1 does not exhibit a typical GPI-signal sequence, containing a 32-amino acid hydrophilic extension in its COOH-terminal end. Here we experimentally demonstrate that the COOH-terminal sequence of hCFC1 functions as a GPI-anchoring signal. Moreover, addition of a hydrophilic epitope tag of 55-amino acids (V5-His) after the GPI signal of hCR-1 interfered with generation of a GPI-anchored form of hCR-1. In contrast, addition of the same epitope tag to the end of GPI signal of hCFC1 did not affect the GPI-attachment of hCFC1. The COOH-terminal signal of hCFC1 could produce two different forms of the protein; a GPI-anchored form and an unprocessed form which was more prone to be secreted into the conditioned medium. The hydrophilic extension of hCFC1 negatively regulates the activity of hCFC1 as a Nodal co-receptor. These results demonstrate the presence of endogenous GPI-signal sequence with a hydrophilic extension, which can generate both GPI-anchored and soluble forms of the protein.

Keywords

Cripto-1; Cryptic; EGF-CFC family protein; GPI-anchored protein; Nodal

INTRODUCTION

Epidermal Growth Factor-Cripto-1/FRL-1/Cryptic (EGF-CFC) family of proteins performs an essential role in vertebrate development and in tumor progression [1, 2]. Two functional members of the EGF-CFC family proteins have been identified in human; Cripto-1 (hCFC2/hCR-1) and Cryptic (hCFC1). Knockout studies of mouse orthologous genes (mCr-1 and

*Author for correspondence: PhD, Bldg37 Rm1118B 37 Convent Drive Bethesda, MD 20892-4254. Tel: +1 301 402 8656; Fax: +1 301 402 8656; salomond@mail.nih.gov.

Publisher's Disclaimer: This is a PDF file of an unedited manuscript that has been accepted for publication. As a service to our customers we are providing this early version of the manuscript. The manuscript will undergo copyediting, typesetting, and review of the resulting proof before it is published in its final citable form. Please note that during the production process errors may be discovered which could affect the content, and all legal disclaimers that apply to the journal pertain.

NIH-PA Author Manuscript
NIH-PA Author Manuscript
NIH-PA Author Manuscript

NIH-PA Author Manuscript

NIH-PA Author Manuscript

NIH-PA Author Manuscript

mcfc1) suggested that these two genes are essential during embryonic development [3–5]. Cr-1-null mice are embryonic lethal at day E8.5–10.5 mainly due to the failure to form appropriate germ layers [3]. On the other hand, mcfc1-null mice are not embryonic lethal but die within first 2 weeks because of severe left-right laterality defects and cardiac malformations [4, 5]. Both CR-1 and CFC1 can function as obligatory co-receptors for the TGFβ family ligand Nodal to facilitate their binding to the Activin type I receptors (ALK) 4/7 and Activin type II receptor [6]. Binding of Nodal to its receptors induces Smad2/3 phosphorylation which can heterodimerize with Smad4 and regulate gene transcription in the presence of the co-transcriptional cofactor Fast-1 (FoxH1) [6].

CR-1 and CFC1 proteins contain NH_2-terminal signal sequences, modified EGF-like domains that bind to Nodal, cysteine-rich CFC domains that bind to ALK4/7 and COOH-terminal hydrophobic domains [1, 2]. The COOH-terminal hydrophobic domain of human and mouse CR-1/Cr-1 has been described as a glycosylphosphatidylinositol (GPI)-attachment signal [7–9] and the COOH-terminal hydrophobic domain of hCFC1 has been also shown to serve as a membrane-anchoring signal [10], even though the GPI-attachment of human CFC1 has not been experimentally demonstrated. The membrane-anchor domain of CFC1 is considered to be important since a frameshift mutation at the beginning of the membrane-associating domain in human *CFC-1* is related to human left-right laterality defects [10].

Biosynthesis of GPI-anchored proteins requires an NH_2-terminal leader sequence and a COOH-terminal GPI signal sequence which is recognized by the GPI transamidase complex and then cleaved during the addition of the GPI moiety [11–13]. The COOH-terminal signal sequences for GPI-attachment are usually 17 to 31 amino acids in length and, in most cases, consist of four regions; 1) an unstructured linker region, 2) a region of small amino acid residues including the ω-site for propeptide cleavage and GPI-attachment, 3) a hydrophilic spacer region, and 4) a hydrophobic tail [11, 14, 15]. These sequences are recognized by the GPI-transamidase complex after translation of the protein core with subsequent addition of GPI and signal peptide cleavage which occurs in the endoplasmic reticulum (ER) [13, 16]. Although previous studies have suggested that artificially generated, internally positioned GPI-signals can be substrates for the GPI-transamidase [17, 18], all known endogenous GPI-anchored proteins contain hydrophilic extensions of no more than a few amino acids [14, 17, 19, 20]. In this context, hCR-1 exhibits a typical sequence of GPI-signal in its COOH-terminus. In contrast, the COOH-terminal sequence of hCFC1 is not a typical GPI-signal sequence since the COOH-terminal sequence of hCFC1 contains an additional 32 amino acids hydrophilic extension (Fig. 1*A*).

We have previously shown that the GPI-anchor of hCR-1 is necessary for optimal biological activity of hCR-1 as a co-receptor to mediate Nodal signaling [9]. Thus, we hypothesized that hCFC1 protein might also be a GPI-anchored even though hCFC1 exhibits an atypical GPI signal sequence. Here we experimentally demonstrate that both hCR-1 and hCFC1 proteins are GPI-anchored proteins and define the different properties of these two GPI-signals. These results describe the presence of an endogenous non-canonical GPI-signal sequence with a hydrophilic extension.

MATERIALS AND METHODS

Cell culture

HEK293T (293T) cells were obtained from ATCC (Manassas, VA) and maintained in Dulbecco's modified Eagle's medium supplemented with 10% fetal bovine serum at 37°C, in 5% CO_2.

NIH-PA Author Manuscript

NIH-PA Author Manuscript

NIH-PA Author Manuscript

Expression vectors and transfection

The cDNA encoding the open reading frame of hCR-1 was previously described [8]. The cDNA encoding the open reading frame of hCFC1 was also cloned from NTERA2/D1 embryonal carcinoma cells in this work and validated by direct sequencing. The obtained sequence of hCFC1 completely matched the reported sequence (Accession number; **AF312769**). All hCR-1- or hCFC1-related constructs except for the FLAG-tagged constructs were cloned into the pEF6/V5-His TOPO TA expression vector (Invitrogen, Carlsbad, CA). A chimeric construct of hCR-1 with the COOH-terminal domain of hCFC1 (CR-CFC) was generated by PCR-based method using primers; hCR-1 start-F, ACCATGGACTGCAGGAAGATG; CR-CFC chimera-F, GCATTTCTACCCGGCTGTATCCGAAAGACTTCCTGGCCTCC; CR-CFC chimera-R, GGAGGCCAGGAAGTCTTTCGGATCACAGCCGGGTAGAAATGC; hCFC1 stop-R, TTAAAGGCGATGCCCAAG. All V5-His tagged constructs were generated from PCR products with reverse primers without a stop codon. FLAG-tagged hCR-1 or hCFC1 constructs were generated with p3xFLAG-Myc-CMV™-24 expression vector (Sigma-Aldrich, St. Louis, MO) which contains a preprotrypsin signal sequence followed by three tandem FLAG sequence at the NH_2-terminus. DsRed-Monomer-Golgi expression vector was purchased from Clontech (Mountain View, CA). Other expression vectors were as previously described [9]. Transfections were performed using Lipofectamine 2000 (Invitrogen) according to the manufacturer's instructions.

Western blot analysis

Total protein (30 μg/well) or conditioned medium (40 μl/well) was resolved on 16% gradient SDS-PAGE gels (Invitrogen) and was transferred to PVDF membrane (Millipore, Temecula, CA). After blocking with 5% milk, hCR-1-related proteins were detected with an anti-hCR-1 mouse monoclonal antibody (mAb) (B3F6, Biogen Idec., Cambridge, MA) at a 1:5000 dilution or with an anti-V5 mouse mAb (Invitrogen) at a 1:5000 dilution and anti-mouse IgG horseradish peroxidase-conjugated secondary antibody (1:3000, Amersham Biosciences, Piscataway, NJ). hCFC1-realted proteins were detected with a sheep anti-hCFC1 polyclonal antibody (R&D Systems, Minneapolis, MN) at a concentration of 0.2 μg/mL and anti-sheep IgG horseradish peroxidase-conjugated secondary antibody (1:3000, Santa Cruz, Santa Cruz, CA). All images of Western blot analysis in this work were visualized, processed, and quantified with Image Analyzer equipped with LabWorks software (Ultra Violet and Laboratory Produces, Upland, CA).

Phosphatidylinositol-phospholipase C (PI-PLC) treatment

Transiently transfected 293T cells were collected with enzyme-free cell dissociation buffer (PBS containing 4 mM EDTA). After washing with PBS, cells were incubated in suspension with PBS containing 1 U/mL of PI-PLC (Sigma-Aldrich, St. Louis, MO) at 37°C for 30 min, unless otherwise specified. Cells were then centrifuged at 10000*g* to divide pellets and supernatants, followed by Western blot or FACS analysis.

FACS analysis

293T cells which had been transiently transfected with CR-1- or CFC1-related expression vectors were collected with enzyme-free cell dissociation buffer and washed with ice-cold FACS buffer (PBS with 0.1% bovine serum albumin and 0.09% sodium azide). For staining of cell-surface hCR-1, 1.0×10^5 cells were incubated for 30 min with Phycoerythrin (PE)-conjugated anti-hCR-1 mAb (FAB 2772P, R&D Systems) at a dilution of 1:50. For staining of cell-surface hCFC1, cells were incubated for 30 min with 50 μg/mL of the sheep anti-hCFC1 polyclonal antibody (R&D Systems), washed with FACS buffer three times, and incubated with anti-sheep IgG Alexa Fluor 488 conjugate (1:50, Invitrogen). Cells were then

NIH-PA Author Manuscript

NIH-PA Author Manuscript

NIH-PA Author Manuscript

pelleted, resuspended in 500 μL of ice-cold FACS buffer, and analyzed using a FACScan instrument (BD Biosciences, San Jose, CA).

[^{3}H]-ethanolamine Metabolic labeling

293T cells were transiently transfected with expression vectors for FLAG-tagged proteins. After 24 h, [^{3}H]-ethanolamine (100 μCi/mL, Amersham) was added to culture medium and the cells were incubated for another 24 h. Cells were washed and lysed in RIPA buffer (10 mM Tris-HCl, pH 8.0, 150 mM NaCl, 1% NP-40, 1% sodium deoxycholate, 0.1% SDS, 10 mM EDTA) with complete protease inhibitor (Roche, Basel, Switzerland). After centrifugation at 14000 rpm, the supernatants were incubated with anti-FLAG M2 conjugated agarose (Sigma-Aldrich) at room temperature for 1 h. The beads were washed with RIPA buffer four times, and immunoprecipitated proteins were eluted with SDS-PAGE sample loading buffer containing 2-mercaptoethanol. After SDS-PAGE, the gel was treated with the EN3HANCE reagent (PerkinElmar, Walthan, MA) to enhance the signal. Autoradiography was performed for 14 days.

Phase separation

Phase separation by Triton X-114 was performed as previously described [8]. Cells were lysed in Triton X-114 solution (20 mM Tris, pH 8.0, 150 mM NaCl, 2% Triton X-114) for 1 h on ice. After removal of cell debris by centrifugation at 14000*g*, phase separation was carried out by warming to 37°C and subsequent centrifugation at 3000*g*, 25°C. The upper aqueous phase and the lower detergent phase were carefully collected by micropipettes. Before applying for Western blotting, proteins were precipitated with Chrolform-Methanol (1:4, v/v) precipitation to remove the detergent.

Immunocytochemistry

293T cells which had been transiently transfected with each CR-1- or CFC1-related expression vector and/or the Golgi marker DsRed-Golgi were seeded in poly-L-lysine (Sigma-Aldrich)-coated 4-well chambered slides 24 h prior to staining. After washing with PBS, cells were fixed in 4% paraformaldehyde and permeabilized with 0.2% Triton X-100. CR-1-related proteins were detected with 5 μg/mL of anti-hCR-1 mAb (MAB2771, R&D Systems) or anti-V5 mAb (Invitrogen) at a 1:200 dilution. For co-staining with anti-hCR-1 mAb (IgG_1) and anti-V5 mAb (IgG_{2a}), samples were first stained with anti-V5 mAb and Alexa Fluor 596-conjugated anti-mouse whole IgG secondary antibody (1:200, Invitrogen) and then stained with anti-hCR-1 mAb and Alexa Fluor 488-conjugated anti-mouse IgG_1-specific secondary antibody (1:200, Invitrogen). hCFC1 protein was stained with 25 μg/mL of the sheep anti-hCFC1 polyclonal antibody (R&D Systems) and anti-sheep IgG Alexa Fluor 488 conjugate (1:200, Invitrogen). For confocal images, a Zeiss LSM 510 NLO Meta confocal system (Carl Zeiss, Oberkochen, Germany) with an Axiovert 200M inverted microscope equipped with a 63× NA 1.4 Plan-Apochromat oil immersion objective lens was used. Z stacks were collected with Zeiss AIM software using a multi-track configuration.

Luciferase assay

Dual luciferase assays were performed as described previously [9]. 293T cells which had been plated in 24-well cell culture plates were transfected with an optimized amount of expression vectors ((n2)7-Luc, 50 ng/well; TK-renilla, 5 ng/well; mouse Fast-1, 25 ng/well; mouse Nodal, 100 ng/well; ALK4-HA, 10 ng/well; hCR-1/hCFC1 variants/mutants, 5–100 ng/well). pEF6/V5-His empty vector (EV) was used as a negative control. After 24 h, dual luciferase assays were carried out using a Dual Luciferase Reporter Assay Kit (Promega, Nadison, WI).

NIH-PA Author Manuscript

NIH-PA Author Manuscript

NIH-PA Author Manuscript

Statistical analysis

Student's *T*-test was used to determine the statistical significance of the quantitative results. Results with a *P* value <0.05 were considered statistically significant.

RESULTS

GPI-anchorage of hCFC1 protein

A majority of EGF-CFC proteins including human CR-1, mouse Cr-1, and mouse cfc1, exhibit typical amino acid sequences for a GPI-attachment signal with possible ω-sites, hydrophilic spacer regions, and hydrophobic domains at the COOH-terminus (Fig. 1*A, B, D, E*). All three proteins (human CR-1, mouse Cr-1, and mouse cfc1) were predicted to be GPI-anchored proteins by a standard prediction program for the GPI-anchored proteins ('big-ΠI predictor') [15]. Unlike other EGF-CFC proteins, hCFC1 contains a 32-amino acid of hydrophilic extension at the COOH-terminal end (Fig. 1*A* and *C*) and was not predicted to be a GPI-anchored protein from its amino acid sequence. To ascertain if the membrane attachment of hCFC1 protein [10] is mediated by GPI-anchoring or by other forms of membrane-anchorage, we analyzed the sensitivity of wild-type hCFC1 to PI-PLC which is a bacterial enzyme widely used to identify GPI-anchored proteins [21] in transiently transfected 293T cells (Fig. 2*A*). PI-PLC treatment released the CFC1 protein. Released proteins showed slower SDS-PAGE mobility as compared to the cell-associated proteins, likely due to the removal of lipid components which exhibit relatively high affinity to SDS (Fig. 2*B*). This mobility shift was generally observed for other GPI-anchored proteins, including CR-1 [8] or an artificial GFP-GPI protein (Supplementary Fig. S1). To confirm the effect of PI-PLC treatment on cell-surface expression of hCFC1, we performed a FACS analysis with or without prior treatment with PI-PLC (Fig. 2*B*). When we analyzed cell-surface expression of hCFC1- or hCR-1-related proteins in transiently transfected 293T cells, two distinct peaks (arrows) were observed which may represent low and high expressing populations in these transiently transfected cells. PI-PLC treatment markedly decreased the cell-surface expression of wild-type CFC1. To directly confirm the GPI-anchorage of human CFC1, we generated NH_2-terminal Flag-tagged expression vectors of CR-1 (Flag-CR-1), transmembrane form of CR-1 (Flag-CR1TM), and CFC1 (Flag-CFC1), and performed the metabolic labeling of GPI-anchorage with [^{3}H]-ethanolamine (Fig. 2*C*). [^{3}H]-ethanolamine was incorporated into Flag-CR-1 and Flag-CFC1 but not into Flag-CR1TM. The different band pattern between the immunoblotting and [^{3}H]-ethanolamine incorporation assays suggests that some of the species were not modified as GPI-anchored proteins. These results strongly suggest the GPI-anchorage of hCFC1 protein.

To compare the functional difference of COOH-terminal GPI signals of hCR-1 and hCFC1 within the same background, we generated a chimeric construct of hCR-1 and the COOH-terminal domain of hCFC1 (CR-CFC) (Fig. 3*A*). We compared the sensitivity of wild-type hCR-1 (CR1WT) and CR-CFC to PI-PLC (Fig. 3*B*). CR1WT and CR-CFC proteins were released into the supernatants after the PI-PLC treatment. FACS analysis confirmed that CR1WT and CR-CFC chimeric proteins were sensitive to PI-PLC treatment, whereas CR1TM, a transmembrane form of hCR-1 was not (Fig. 3*C*). These results suggest that both GPI signal sequences of hCR-1 and hCFC1 are functional in the same background.

Effect of COOH-terminal addition of a hydrophilic peptide tag on GPI-anchorage of hCR-1 and hCFC1

Previous reports demonstrated that a GPI-signal can function even when a hydrophilic sequence is artificially introduced after the hydrophobic segment [17, 18]. However, we have demonstrated that addition of an artificial sequence after the COOH-terminal GPI signal of hCR-1 interfered with the correct localization and biological activity of the hCR-1

NIH-PA Author Manuscript

NIH-PA Author Manuscript

NIH-PA Author Manuscript

protein [9]. In order to address if an artificial extension of hydrophilic amino acid sequences might affect the GPI-attachment in hCFC1 as well as hCR-1, we introduced a V5-His tag that consists of 55 amino acids of which a majority is hydrophilic amino acids at the COOH-terminal end of hCR-1 and hCFC1 (Fig. 4*A*). We analyzed the effect of this artificial extension to COOH-terminus using CR-1 and CR-CFC chimeric proteins in order to compare within the same background. Western blot analysis of cell lysates using a hCR-1-specific mAb which recognizes an epitope in the NH_2-terminal region of hCR-1 [22] revealed that CR1WT protein was primarily produced in two major forms (~26-kD and ~24-kD forms) and a minor ~18-kD fragment and the CR-CFC chimeric protein was produced in three major forms (~28-kD, ~25-kD and ~23-kD forms) (Fig. 4*B*). In a COOH-terminal V5-His tagged form of hCR-1 (CR1-V5), only one major band (~30 kD) was observed. In contrast, the COOH-terminal V5-His tagged form of CR-CFC (CR-CFC-V5) was detected as three major forms (~38-kD, ~25-kD and ~23-kD forms) of which the smaller two bands were identical to those of CR-CFC protein (~25-kD and ~23-kD forms). Immunoblot analysis of the CR1-V5 protein with anti-V5 antibody detected only a ~30-kD band which was identical to the form that was detected by the anti-hCR-1 mAb, suggesting that the cleavage of COOH-signal does not occur in CR1-V5 at a detectable level (Fig. 4*B*). In contrast, only the ~38-kD form of CR-CFC-V5 was detected with an anti-V5 antibody but this antibody did not recognize ~25-kD or ~23-kD forms of CR-CFC-V5. These results suggest that the ~25-kD and ~23-kD forms of CR-CFC and CR-CFC-V5 are the products after cleavage of the COOH-terminal signal and probably have been processed for GPI-anchor attachment, since the removal of GPI signal sequence of the precursor proteins and its replacement with GPI moiety are mediated by a catalytic subunit of the GPI transamidase (GPI8) and occur simultaneously [13, 16]. Western blotting of the conditioned medium revealed that the unprocessed form of CR-CFC and CR-CFC-V5 (~28-kD form of CR-CFC and ~38-kD form of CR-CFC-V5, respectively) were more abundant than the processed forms, whereas lesser amounts of CR1WT and none of CR1-V5 were detected in the conditioned medium (Fig. 4*C*). Much higher amounts of the COOH-terminally truncated form of hCR-1 (CR1ΔC) were secreted into the conditioned medium as previously described [9]. This suggests that the unprocessed forms of CR-CFC and CR-CFC-V5 do not possess a GPI-anchor and possibly are directly shunted through a secretory pathway. We then performed Triton-X114 phase partitioning in order to characterize the hydrophobicity of each species of these CR-1/CFC1 variants (Fig. 4*D*). As described previously [8], CR1WT was mainly partitioned into the detergent phase, suggesting the hydrophobic characteristics of the CR1WT protein. CR1-V5 was more abundant in the aqueous phase. For the CR-CFC and CR-CFC-V5 proteins, substantial amounts of unprocessed forms (~28-kD form of CR-CFC and ~38-kD form of CR-CFC-V5, respectively) were detected in the aqueous phase whereas the smaller forms (~25-kD and ~23-kD of both variants) were mainly partitioned into the detergent phase. In addition, PI-PLC treatment released only the smaller forms (~25-kD and ~23-kD of CR-CFC and CR-CFC-V5) into the supernatants (Fig. 4*E*). These data strongly support the possibility that the ~25-kD and ~23-kD forms of CR-CFC and CR-CFC-V5 are processed, GPI-anchored forms.

We then assessed for the cell-surface expression of each variant form of hCR-1 by FACS analysis in transiently transfected 293T cells (Fig. 5). Cell-surface expression of CR1-V5 was significantly reduced compared with that of CR1WT (Fig. 5*A*). On the other hand, CR-CFC-V5 showed a comparable level of cell-surface expression with CR-CFC (Fig. 5*B*). PI-PLC treatment completely abolished the cell-surface signal of CR1-V5 (Fig. 5*C*), suggesting that a small fraction of the CR1-V5 protein could exist as a GPI-anchored form, even though the level is extremely low as compared to the CR1WT protein. This observation is consistent with the previous report that demonstrated an internally positioned GPI-signal can produce GPI-anchored proteins with reduced efficiency [17]. The cell-surface expression of CR-

NIH-PA Author Manuscript

NIH-PA Author Manuscript

NIH-PA Author Manuscript

CFC-V5 was also reduced after PI-PLC treatment (Fig. 5*D*) similar to that observed for CR-CFC (Fig. 2*D*).

To ascertain if these results observed in CR-CFC chimeric background can be observed in hCFC1 background, we utilized Flag-tagged expression vectors for CR-1, CFC1, and CFC1-V5. Western blot analysis of cell lysates detected similar band patterns with Flag-tagged forms of CR-1, CFC1 and CFC1-V5 (Fig. 6*A*), as compared to the non-tagged forms of proteins (Fig. 4), respectively. We also detected strong signals for the unprocessed, larger forms of Flag-CFC1 and Flag-CFC1-V5 in the conditioned medium, and faint signals were detected for the mature forms of Flag-CR-1, Flag-CFC1, and FLAG-CFC1-V5 (Fig. 6*B*). We then directly addressed the GPI-anchorage of Flag-CFC1, and Flag-CFC1-V5 by metabolic labeling with [^{3}H]-ethanolamine (Fig. 6*C*). [^{3}H]-ethanolamine was equally incorporated into Flag-CFC1, and Flag-CFC1-V5, and showed identical band patterns, suggesting that the mature forms of CFC1 protein produced from both constructs were identical.

We then assessed the intracellular localization of the COOH-terminal variant forms of hCR-1 and hCFC1 by a confocal microscopy. The CR1WT protein was detected on the plasma membrane as well as in intracellular Golgi as assessed by co-transfection with DsRed-Golgi and staining with an anti-hCR-1 mAb (Fig. 7*A*), as previously described [9]. The CR-CFC and CR-CFC-V5 proteins showed almost identical staining patterns to the CR1WT protein (Fig. 7*B* and *D*). In contrast, the CR1-V5 protein showed an aberrant cytoplasmic punctate staining which was not associated with Golgi in most cases (Fig. 7*C*). The cell-surface localization of CR1-V5 was not detectable by immunocytochemical analysis, even though a weak cell-surface signal of CR1-V5 was detected by FACS analysis (Fig. 5*A*), which is likely due to different sensitivity between these two assays. When the expressed proteins were visualized with an anti-V5 antibody, CR1-V5 protein was found to localize in cytoplasmic regions which were not associated with Golgi (Fig. 7*E*) and the CR-CFC-V5 protein showed a trans-Golgi network pattern without plasma membrane staining (Fig. 7*F*). The staining pattern of the CR1-V5 protein with the anti-V5 antibody completely overlapped with the pattern that was detected by the anti-hCR-1 mAb which can recognize a NH2-terminal epitope in hCR-1 (Fig. 7*G*). In contrast, the membrane localization of CR-CFC-V5 was detectable only with anti-hCR-1 mAb but not with the anti-V5 antibody (Fig. 7*H*). These results suggest that only the COOH-terminally processed form(s) of CR-CFC-V5 can be expressed on the cell surface, confirming that only the products after cleavage of the COOH-terminal signal are processed for GPI-attachment and expressed on plasma membrane (Fig. 4). The CFC1WT protein showed a plasma membrane and Golgi localization pattern that was similar to the CR1WT protein (Fig. 7*I*). CFC1-V5 protein was stained differently with the anti-CFC1 antibody and the anti-V5 antibody (Fig. 7J). V5-tag was only detected in intracellular Golgi-like structure (Fig. 7J), as observed in CR-CFC-V5 protein (Fig. 7*F* and *H*)

To determine the biological activity of the COOH-terminal variants of hCR-1 and hCFC1 as Nodal co-receptors, we analyzed the activity of the expressed proteins in 293T cells using the Activin/Nodal-responsive (n2)7-luciferase reporter [(n2)7-Luc] (Fig. 8), which contains mouse Fast-1 binding sites from the *Nodal* left side-specific enhancer [23]. Reporter assays were performed as previously described [9]. The CR1-V5 protein lost significant activity to induce Nodal signaling as compared to the CR1WT protein, whereas the activity of V5-tagged hCFC1 (CFC1-V5) and CR-CFC-V5 were comparable to that of CFC1WT and CR-CFC, respectively. Importantly, wild-type hCFC1 (CFC1WT) showed a 50% reduction in activity as compared to wild-type hCR1 (CR1WT) with respect to mediating Nodal induced reporter activation in accordance with the precious report [24]. These results suggest that the addition of an artificial sequence at the COOH-terminus did not affect the processing or

NIH-PA Author Manuscript

NIH-PA Author Manuscript

NIH-PA Author Manuscript

functional activity for the GPI-signal of hCFC1, but did reduce the efficiency of processing and activity for that of the hCR-1 protein.

Functional role of the COOH-terminal hydrophilic extension of hCFC1 in Nodal signaling

To ascertain if the COOH-terminal hydrophilic extension of hCFC1 might have any functional significance, we generated a COOH-terminally truncated construct of CR-CFC (CR-CFC L191stop) in which the 32 amino acids of COOH-terminal hydrophilic extension were deleted (Fig. 9*A*). We also generated the V5-His tagged form of CR-CFC L191stop (CR-CFC L191-V5) (Fig. 9*A*). Western blot analysis of these COOH-terminally truncated forms of CR-CFC revealed that the CR-CFC L191stop variant produced two major bands of ~25-kD and ~23-kD of GPI-processed forms and the CR-CFC L191-V5 variant protein was processed to ~25-kD and ~23-kD GPI-processed forms and an unprocessed ~30-kD form which was also detected by anti-V5 antibody (Fig. 9*B*, CL). The GPI-processed forms (~25-kD and ~23-kD forms) are similar to these observed in CR-CFC or CR-CFC-V5 proteins (Fig. 9*B*, CL). In the conditioned medium, the unprocessed ~30-kD form of the CR-CFC L191-V5 protein was detected at a similar level as the unprocessed ~28-kD form of the CR-CFC protein and the unprocessed ~38-kD form of the CR-CFC-V5 protein (Fig. 9*B*, CM). Lesser amounts of the CR-CFC L191stop protein as compared to the unprocessed forms of the CR-CFC, CR-CFC-V5 or CR-CFC L191-V5 protein were found in the conditioned medium (Fig. 9*B*, CM) which was similar to that observed for the CR1WT protein as compared to the unprocessed form of the CR-CFC or CR-CFC-V5 protein (Fig. 4*C*). FACS analysis revealed that the cell-surface expression of both CR-CFC L191stop and CR-CFC L191-V5 proteins were similar to that of the CR-CFC protein (Fig. 9*C*). A similar membrane and Golgi localization to the CR-CFC protein was observed with the CR-CFC L191stop and CR-CFC L191-V5 proteins as detected by immunofluorescent analysis (Fig. 9*D* and *E*). In CR-CFC L191-V5, only perinuclear trans-Golgi but not plasma membrane detection was observed using the anti-V5 antibody (Fig. 9*F*), confirming that the V5-tag containing ~30-kD form of CR-CFC L191-V5 (Fig. 9*B*) has not been processed to a GPI-anchored membrane protein. We then assessed the biological activity of these COOH-terminally truncated forms of CR-CFC to mediate Nodal-dependent signaling with the (n2)7-Luc reporter assay (Fig. 9*G*). The CR-CFC L191-V5 variant showed similar activity to induce Nodal signaling as the CR-CFC construct, whereas the CR-CFC L191stop variant exhibited significantly higher activity than the CR-CFC construct. The co-receptor activity of the CR-CFC L191stop variant was comparable with that of the CR1WT protein. A comparable negative effect of the hydrophilic extension was also observed in the original CFC1 construct. When the hydrophilic region was removed the ability of the CFC1 protein to mediate Nodal dependent signaling or a co-receptor increased (CFC1WT versus CFC1 L191stop, Fig. 9*G*). These results suggest that the hydrophilic extension of hCFC1 may negatively regulate the biological activity of hCFC1 to induce Nodal signaling possibly by reducing efficiency to produce a functional GPI-anchored protein.

DISCUSSION

Previous data from our laboratory suggested that GPI-anchorage of hCR-1 is necessary for optimal biological activity of the protein as a Nodal co-receptor to mediate Nodal dependent signaling [9]. In the present study, we experimentally demonstrated that hCFC1, a member of EGF-CFC proteins and a close relative to hCR-1, is also a GPI-anchored protein, even though hCFC1 does not exhibit a typical GPI-signal sequence in the COOH-terminus. Although previous studies implicated that a GPI-signal can be recognized even when the signal is positioned internally [17, 18], all endogenous GPI-anchored proteins reported to date contain a hydrophobic domain at the COOH-terminal end except for a few amino acid extension [14, 17, 19, 20]. In this context, GPI-signal of hCFC1 is a noncanonical

NIH-PA Author Manuscript

NIH-PA Author Manuscript

NIH-PA Author Manuscript

endogenous GPI-signal which contains a long 32-amino acid hydrophilic extension at the COOH-terminus. This suggests that other GPI-anchored proteins might exist, which do not exhibit a canonical GPI-signal at the extreme COOH-terminal end of the protein. In fact, when we tested the whole sequence of hCFC1 by three web-based *in silico* prediction programs ('big-Π predictor', 'DGPI', and 'GPI-SOM' [20]), none of these programs was able to predict hCFC1 as a GPI-anchored protein. However, when we assessed the sequence of hCFC1 without the 32-amino acid hydrophilic COOH-terminal extension (a.a. 1–191), all of these programs predicted hCFC1 as a GPI-anchored protein. Since most of the current algorithms for prediction of GPI-anchored proteins rely on the core sequences surrounding the ω-site as well as the physiochemical property of GPI-signal peptides including average hydrophobicity of the COOH-terminal segments [15, 19, 20], these programs could be modified to include internally positioned GPI-signals.

A similar hydrophilic extension is found in the CFC1 orthologue in chimpanzee (Accession number; **XP_001144170**). Other CFC1 orthlogues registered in the NCBI database to date including mouse, rat, and chicken do not contain this hydrophilic extension and exhibit typical GPI-signals with hydrophobic segments at the COOH-terminal end. This suggests that the hydrophilic extension of primate hCFC1 proteins have diverged in evolution for a yet unknown function. Substitution of this hydrophilic sequence with non-specific hydrophilic sequence such as a V5-His tag (CR-CFC L191-V5) did not affect the localization and biological activity of the CFC1 protein, suggesting that the hydrophilic extension does not have to be a specific sequence, which is consistent with previous observations [17, 18]. In contrast, the COOH-terminal addition of the same V5-His tag sequence to the GPI signal sequence of hCR-1 markedly altered the localization and decreased the biological activity of the hCR-1 protein to function as a Nodal co-receptor. This suggests that some GPI-signal sequences can tolerate the addition of a hydrophilic extension but that others can not. In fact, the hydrophobic domain of hCFC1 and mcfc1 contain a leucine repeat that is longer than that of hCR-1 or mCr-1 (Fig. 1). It is likely that the length and the degree of hydrophobicity of the hydrophobic segments of the GPI-signal may determine the efficiency of recognition by the GPI-transamidase and GPI-processing.

The significance of the hydrophilic amino acid extension in modulating the biological activity of human CFC1 *in vivo* during development is unclear. However, the present results suggest that this hydrophilic extension may negatively regulate the activity of hCFC1 as a Nodal co-receptor, and may possibly contribute to the fine tuning of the intensity of Nodal signaling to establish the precise body patterning. Moreover, the COOH-terminally epitope-tagged hCFC1 may enable *in situ* tracking of the GPI-signal peptide and may serve as a model system to study the biosynthesis of other GPI-anchored proteins.

Supplementary Material

Refer to Web version on PubMed Central for supplementary material.

Acknowledgments

We dedicate this manuscript to the memory Ms. Brenda W. Jones who assisted during the inception of this research. We thank Ms. Susan Garfield and Mr. Stephen Wincovitch (Confocal Core facility, National Cancer Institute) for help in confocal imaging. This work was supported by NIH Intramural Funding.

Abbreviations used

ALK	activin-like kinase

NIH-PA Author Manuscript

NIH-PA Author Manuscript

NIH-PA Author Manuscript

CR-1	Cripto-1
CFC1	Cryptic
EGF-CFC	Epidermal Growth Factor-Cripto-1/FRL-1/Cryptic
EV	empty vector
GPI	glycosylphosphatidylinositol

REFFERENCES

1. Salomon DS, Bianco C, Ebert AD, Khan NI, De Santis M, Normanno N, Wechselberger C, Seno M, Williams K, Sanicola M, Foley S, Gullick WJ, Persico G. The EGF-CFC family: novel epidermal growth factor-related proteins in development and cancer. Endocr Relat Cancer. 2000; 7:199–226. [PubMed: 11174844]
2. Bianco C, Strizzi L, Normanno N, Khan N, Salomon DS. Cripto-1: an oncofetal gene with many faces. Curr Top Dev Biol. 2005; 67:85–133. [PubMed: 15949532]
3. Ding J, Yang L, Yan YT, Chen A, Desai N, Wynshaw-Boris A, Shen MM. Cripto is required for correct orientation of the anterior-posterior axis in the mouse embryo. Nature. 1998; 395:702–707. [PubMed: 9790191]
4. Gaio U, Schweickert A, Fischer A, Garratt AN, Muller T, Ozcelik C, Lankes W, Strehle M, Britsch S, Blum M, Birchmeier C. A role of the cryptic gene in the correct establishment of the left-right axis. Curr Biol. 1999; 9:1339–1342. [PubMed: 10574770]
5. Yan YT, Gritsman K, Ding J, Burdine RD, Corrales JD, Price SM, Talbot WS, Schier AF, Shen MM. Conserved requirement for EGF-CFC genes in vertebrate left-right axis formation. Genes & development. 1999; 13:2527–2537. [PubMed: 10521397]
6. Shen MM. Nodal signaling: developmental roles and regulation. Development (Cambridge, England). 2007; 134:1023–1034.
7. Minchiotti G, Parisi S, Liguori G, Signore M, Lania G, Adamson ED, Lago CT, Persico MG. Membrane-anchorage of Cripto protein by glycosylphosphatidylinositol and its distribution during early mouse development. Mech Dev. 2000; 90:133–142. [PubMed: 10640699]
8. Watanabe K, Bianco C, Strizzi L, Hamada S, Mancino M, Bailly V, Mo W, Wen D, Miatkowski K, Gonzales M, Sanicola M, Seno M, Salomon DS. Growth factor induction of cripto-1 shedding by GPI-phospholipase D and enhancement of endothelial cell migration. J Biol Chem. 2007
9. Watanabe K, Hamada S, Bianco C, Mancino M, Nagaoka T, Gonzales M, Bailly V, Strizzi L, Salomon DS. Requirement of glycosylphosphatidylinositol anchor of cripto-1 for ‘trans’ activity as a nodal co-receptor. J Biol Chem. 2007
10. Bamford RN, Roessler E, Burdine RD, Saplakoglu U, dela Cruz J, Splitt M, Goodship JA, Towbin J, Bowers P, Ferrero GB, Marino B, Schier AF, Shen MM, Muenke M, Casey B. Loss-of-function mutations in the EGF-CFC gene CFC1 are associated with human left-right laterality defects. Nat Genet. 2000; 26:365–369. [PubMed: 11062482]
11. Eisenhaber B, Maurer-Stroh S, Novatchkova M, Schneider G, Eisenhaber F. Enzymes and auxiliary factors for GPI lipid anchor biosynthesis and post-translational transfer to proteins. Bioessays. 2003; 25:367–385. [PubMed: 12655644]
12. Pittet M, Conzelmann A. Biosynthesis and function of GPI proteins in the yeast Saccharomyces cerevisiae. Biochimica et biophysica acta. 2007; 1771:405–420. [PubMed: 16859984]
13. Orlean P, Menon AK. Thematic review series: lipid posttranslational modifications. GPI anchoring of protein in yeast and mammalian cells, or: how we learned to stop worrying and love glycophospholipids. Journal of lipid research. 2007; 48:993–1011. [PubMed: 17361015]
14. Ikezawa H. Glycosylphosphatidylinositol (GPI)-anchored proteins. Biol Pharm Bull. 2002; 25:409–417. [PubMed: 11995915]
15. Eisenhaber B, Bork P, Eisenhaber F. Prediction of potential GPI-modification sites in proprotein sequences. Journal of molecular biology. 1999; 292:741–758. [PubMed: 10497036]

NIH-PA Author Manuscript

NIH-PA Author Manuscript

NIH-PA Author Manuscript

16. Zacks MA, Garg N. Recent developments in the molecular, biochemical and functional characterization of GPI8 and the GPI-anchoring mechanism [review]. Molecular membrane biology. 2006; 23:209–225. [PubMed: 16785205]

17. Caras IW. An internally positioned signal can direct attachment of a glycophospholipid membrane anchor. J Cell Biol. 1991; 113:77–85. [PubMed: 1706725]

18. Vidugiriene J, Vainauskas S, Johnson AE, Menon AK. Endoplasmic reticulum proteins involved in glycosylphosphatidylinositol-anchor attachment: photocrosslinking studies in a cell-free system. European journal of biochemistry/FEBS. 2001; 268:2290–2300. [PubMed: 11298746]

19. Eisenhaber F, Eisenhaber B, Kubina W, Maurer-Stroh S, Neuberger G, Schneider G, Wildpaner M. Prediction of lipid posttranslational modifications and localization signals from protein sequences: big-Pi, NMT and PTS1. Nucleic acids research. 2003; 31:3631–3634. [PubMed: 12824382]

20. Fankhauser N, Maser P. Identification of GPI anchor attachment signals by a Kohonen self-organizing map. Bioinformatics (Oxford, England). 2005; 21:1846–1852.

21. Sharom FJ, Lehto MT. Glycosylphosphatidylinositol-anchored proteins: structure, function, and cleavage by phosphatidylinositol-specific phospholipase C. Biochemistry and cell biology = Biochimie et biologie cellulaire. 2002; 80:535–549. [PubMed: 12440695]

22. Adkins HB, Bianco C, Schiffer SG, Rayhorn P, Zafari M, Cheung AE, Orozco O, Olson D, De Luca A, Chen LL, Miatkowski K, Benjamin C, Normanno N, Williams KP, Jarpe M, LePage D, Salomon D, Sanicola M. Antibody blockade of the Cripto CFC domain suppresses tumor cell growth in vivo. J Clin Invest. 2003; 112:575–587. [PubMed: 12925698]

23. Saijoh Y, Adachi H, Sakuma R, Yeo CY, Yashiro K, Watanabe M, Hashiguchi H, Mochida K, Ohishi S, Kawabata M, Miyazono K, Whitman M, Hamada H. Left-right asymmetric expression of lefty2 and nodal is induced by a signaling pathway that includes the transcription factor FAST2. Mol Cell. 2000; 5:35–47. [PubMed: 10678167]

24. Yan YT, Liu JJ, Luo Y, Haltiwanger CERS, Abate-Shen C, Shen MM. Dual roles of Cripto as a ligand and coreceptor in the nodal signaling pathway. Mol Cell Biol. 2002; 22:4439–4449. [PubMed: 12052855]

NIH-PA Author Manuscript

NIH-PA Author Manuscript

NIH-PA Author Manuscript

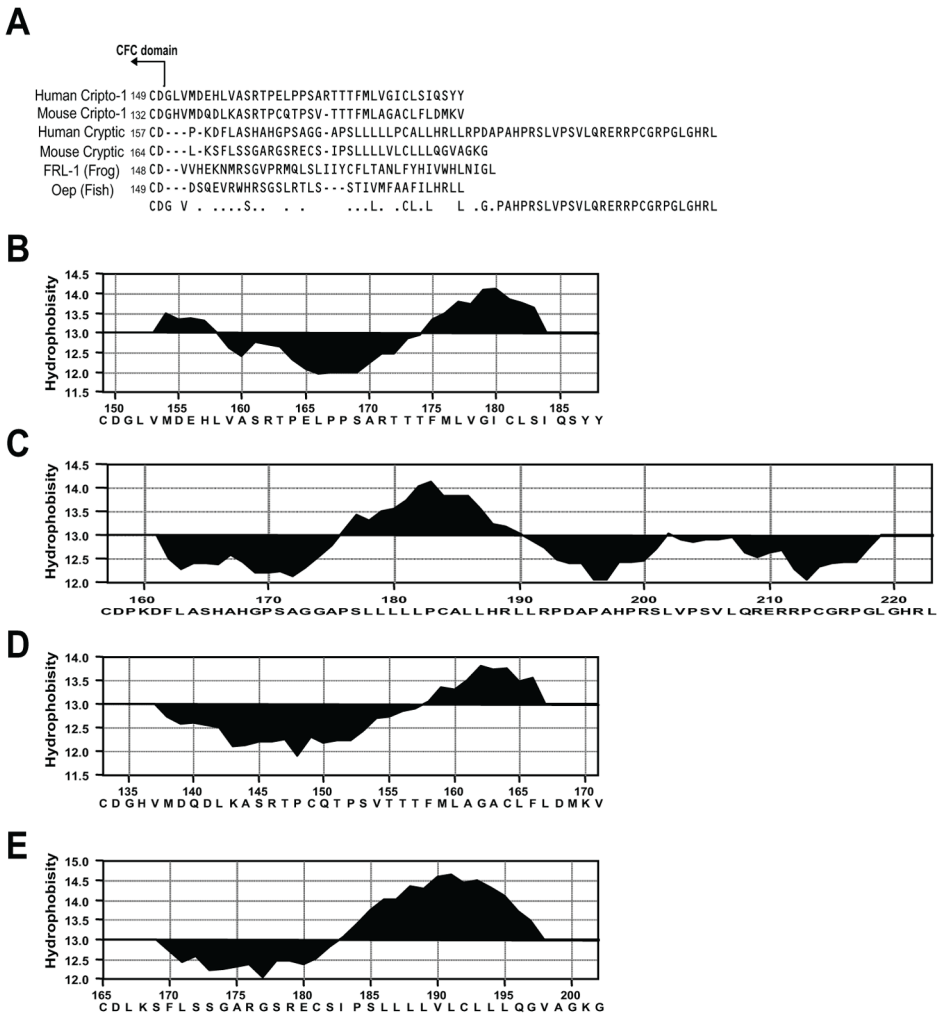

Fig. 1. Sequence analysis of COOH-terminal domains of EGF-CFC proteins

(**A**) Sequences of GPI signal of EGF-CFC proteins. COOH-terminal sequences of indicated gene products are aligned using MacVector software. Conserved amino acids are shown at the bottom. (**B–E**) Hydropathy plot of the human CR-1 (**B**), human CFC1 (**C**), mouse Cr-1 (**D**), and mouse cfc1 (**E**). Hydrophobic scores were determined using the Manavalan algorithm with a window size of 11.

NIH-PA Author Manuscript

NIH-PA Author Manuscript

NIH-PA Author Manuscript

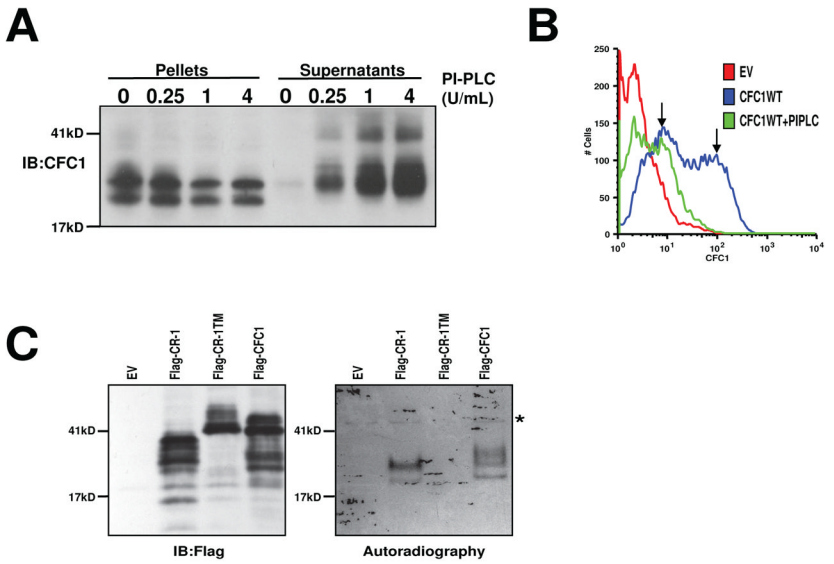

Fig. 2. GPI-attachment of hCFC-1 protein

(**A**) Effect of PI-PLC on release of wild-type hCFC1. 293T cells transiently transfected with the hCFC1 expression vector were collected with enzyme-free cell dissociation buffer and incubated in PBS with the indicated concentration of PI-PLC at 37°C for 30 min. After centrifugation, cells and supernatants were collected and Western blot analysis was carried out using an anti-human CFC1 polyclonal antibody. (**B**) FACS analysis of cell-surface expression of hCFC1 in transiently transfected 293T cells with or without PI-PLC treatment. 293T cells transfected with the indicated constructs were collected and treated with or without PI-PLC (1 unit/mL). After centrifugation, cells were stained with an anti-human CFC1 polyclonal antibody and Alexa Fluor 488-conjugated secondary antibody, and FACS analysis was performed. Arrows indicate the two peaks of the high and low expression population. (**C**) [^{3}H]-ethanolamine Metabolic labeling. 293T cells were transiently transfected with indicated constructs and labeled with [^{3}H]-ethanolamine (100 μCi) for 24 h. The cell lysates were subjected to immunoprecipitation using anti-FLAG M2-conjugated agarose. After dissolving on SDS-PAGE, the samples were analyzed by autoradiography. *; non-specific bands.

NIH-PA Author Manuscript

NIH-PA Author Manuscript

NIH-PA Author Manuscript

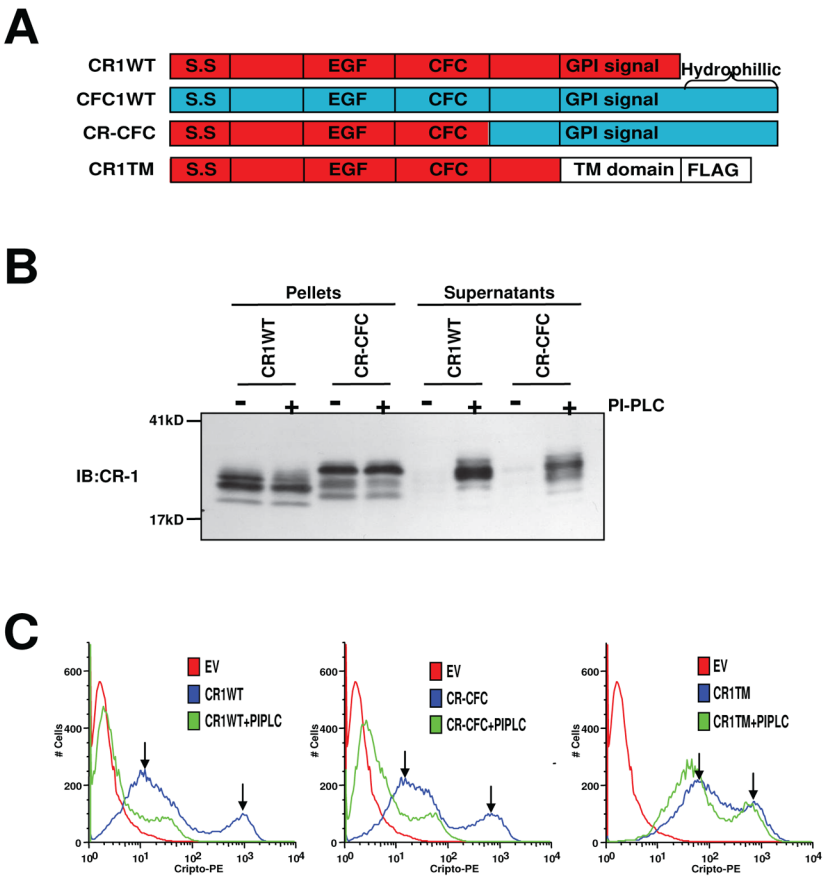

Fig. 3. Generation of a chimeric construct of hCR-1 with GPI signal sequence of hCFC1

(**A**) Schematic of hCR-1 (CR1WT), hCFC1 (CFC1WT), a chimeric construct (CR-CFC), and a transmembrane form of hCR-1 (CR1TM). Sequences from hCR-1 are shown in red and from hCFC1 in blue. (**B**) Effect of PI-PLC on release of CR1WT and CR-CFC. 293T cells were transiently transfected with indicated constructs and PI-PLC treatment (1 unit/mL) was performed. Cells and supernatants were collected and analyzed by Western blotting with an anti-CR-1 specific mAb. (**C**) FACS analysis of cell-surface expression of CR-1 variants in transiently transfected 293T cells with or without PI-PLC treatment. 293T cells transfected with the indicated constructs were collected and treated with or without PI-PLC (1 unit/mL). Cells were stained with PE-conjugated anti-hCR-1 mAb followed by FACS analysis. Arrows indicate the two peaks of the high and low expression population in CR1WT, CR-CFC and CR1TM, respectively.

NIH-PA Author Manuscript

NIH-PA Author Manuscript

NIH-PA Author Manuscript

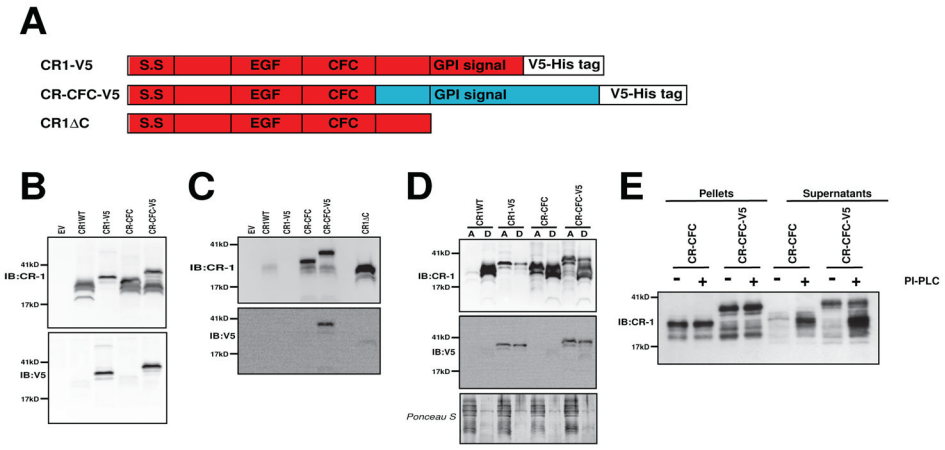

Fig. 4. Protein analysis of COOH-terminal variant forms of hCR-1

(**A**) Schematic of COOH-terminal V5-His-tagged hCR-1 (CR1-V5), CR-CFC (CR-CFC-V5) and a soluble form of hCR-1 (CR1ΔC). Sequences from hCR-1 are shown in red and from hCFC1 in blue. (**B–C**) Western blot analysis of cell lysates (**B**) and conditioned medium (**C**) from 293T cells which had been transiently transfected with indicated constructs. Immunoblot was performed with anti-hCR-1 mAb (upper panel) and the same blots were then stripped and reblotted with an anti-V5 mAb (lower panel). (**D**) Triton-X114 phase separation analysis of cell lysates from 293T cells which had been transfected with indicated constructs. Triton-X114 phase separation was carried out as described in *Materials and Methods*, and aqueous phase (A) and detergent phase (D) were analyzed by Western blotting. Immunoblot was performed with the anti-hCR-1 mAb (upper panel) and the same blots were then stripped and reblotted with the anti-V5 mAb (middle panel). *Ponceau S* staining of the same blot is shown in the bottom. (**D**) Effect of PI-PLC on release of CR-CFC and CR-CFC-V5. 293T cells were transiently transfected with the indicated constructs and PI-PLC treatment (1 unit/mL) was performed. Cells and supernatants were collected and analyzed by Western blotting with an anti-CR-1 specific mAb.

NIH-PA Author Manuscript

NIH-PA Author Manuscript

NIH-PA Author Manuscript

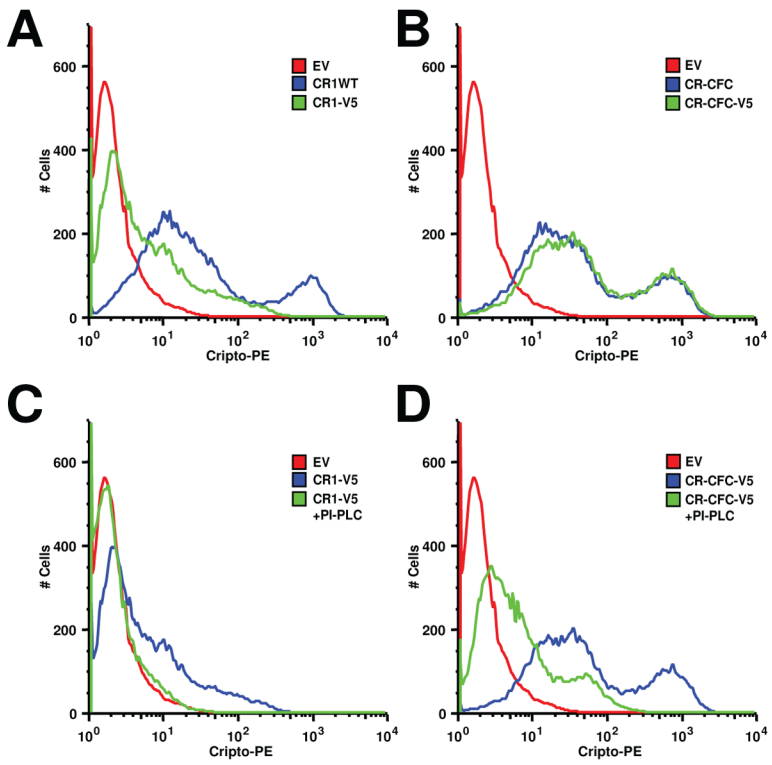

Fig. 5. FACS analysis of cell-surface expression of hCR-1 variants in transiently transfected 293T cells with or without PI-PLC treatment

(**A–B**) Comparison of the cell-surface expression of CR1WT and CR1-V5 (**A**) or CR-CFC and CR-CFC-V5 (**B**) in transiently transfected 293T cells. (**C–D**) 293T cells which had been transiently transfected with CR1-V5 (**C**) or CR-CFC-V5 (**D**) were collected with enzyme-free cell dissociation buffer and incubated in PBS with or without 1 unit/mL PI-PLC at 37°C for 30 min. After centrifugation, cells were collected and stained with PE-conjugated anti-hCR-1 mAb followed by FACS analysis. Empty vector (EV) was used for a negative control.

NIH-PA Author Manuscript

NIH-PA Author Manuscript

NIH-PA Author Manuscript

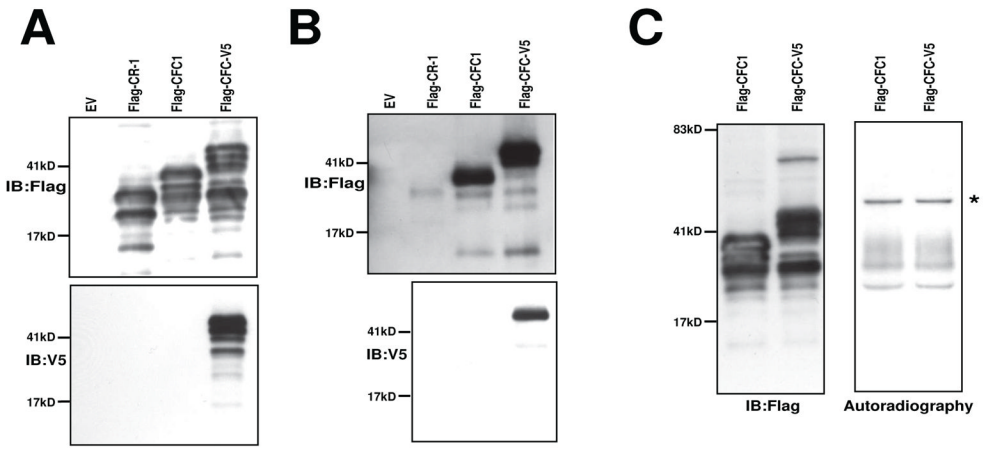

Fig. 6. Protein analysis of Flag-tagged hCFC1 variants

(**A–B**) Western blot analysis of cell lysates (**A**) and conditioned medium (**B**) from transiently transfected 293T cells. Immunoblot was performed with anti-FLAG mAb (upper panel) and the same blots were then stripped and reblotted with an anti-V5 mAb (lower panel). (**D**) [^{3}H]-ethanolamine Metabolic labeling. 293T cells were transiently transfected with indicated constructs and labeled with [^{3}H]-ethanolamine (100 μCi) for 24 h. The cell lysates were subjected to immunoprecipitation using anti-Flag M2-conjugated agarose. After dissolving on SDS-PAGE, the samples were analyzed by autoradiography. *; non-specific bands.

NIH-PA Author Manuscript
NIH-PA Author Manuscript
NIH-PA Author Manuscript

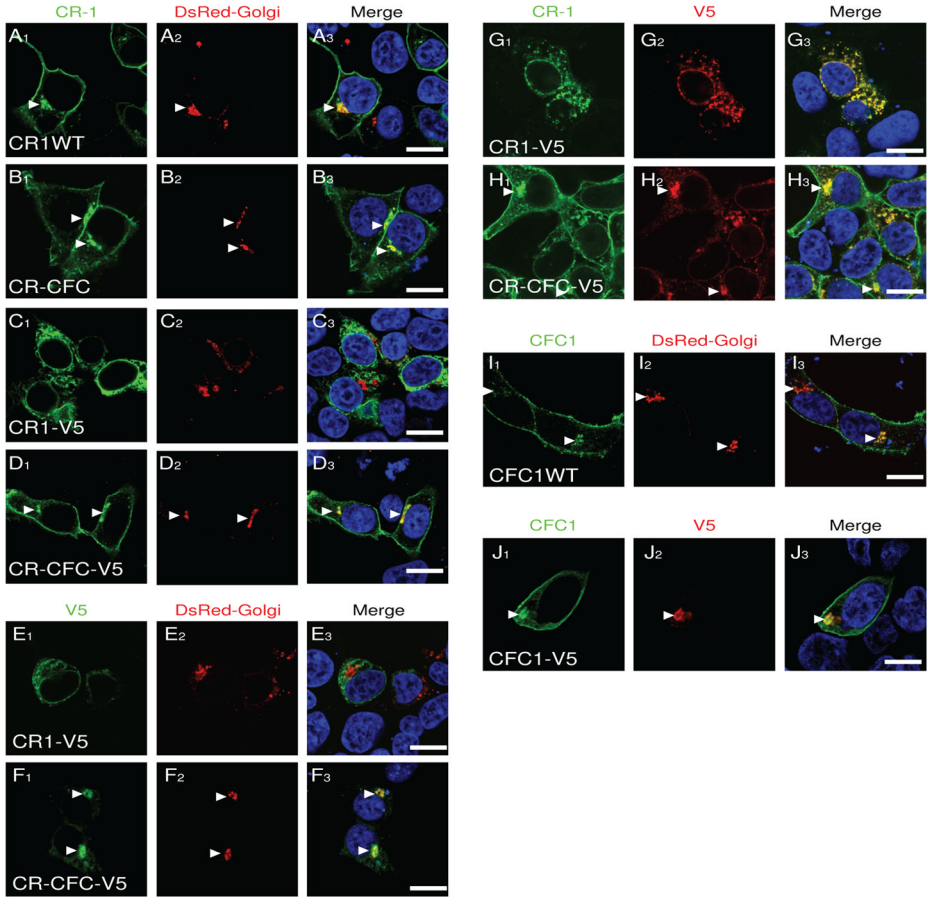

Fig. 7. Subcellular localization of hCR-1/hCFC1 variants in the COOH-terminal domain

(**A–H**) Immunocytochemistry of indicated hCR-1 variants in transiently transfected 293T cells was performed after permeabilization by Triton X-100. CR-1 proteins were stained with anti-CR-1 mAb (**A_1–D_1**, green) or anti-V5 antibody (**E_1–F_1**, green). DsRed-Golgi was co-transfected in **A_2–F_2** (red). Co-staining of V5-tagged constructs with anti-CR-1 mAb (**G_1–H_1**, green) and anti-V5 antibody (**G_2–H_2**, red) is shown in G and H. Nuclei were counterstained with DAPI (blue) and tricolor merged images are shown in **A_3–H_3**. Images were visualized by confocal microscopy. Arrowheads indicate Golgi localization of CR-1 variant protein. Scale bar = 10 μm. (**I–J**) Immunocytochemistry of hCFC1 and CFC1-V5 in transiently transfected 293T cells was performed using anti-human CFC1 specific antibody and anti-V5 mAb. DsRed-Golgi was co-transfected in **I_2** (red). Arrowheads indicate Golgi localization of CFC1 or CFC1-V5 proteins.

NIH-PA Author Manuscript

NIH-PA Author Manuscript

NIH-PA Author Manuscript

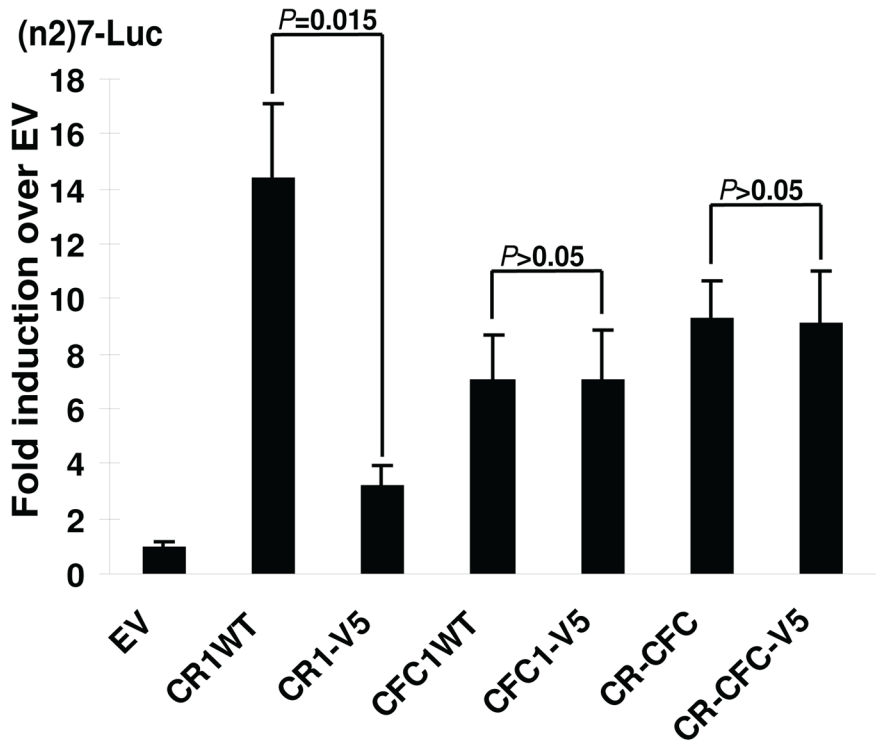

Fig. 8. Co-receptor activities of hCR-1 and hCFC1 variants to mediate Nodal-signaling pathway

Serum starved 293T cells were transiently transfected with the (n2)7-Luc reporter, TK renilla reporter, mFast-1, mNodal-V5, ALK4-HA expression vector and the indicated expression vectors and dual luciferase assay was performed. Values indicate fold induction of relative luciferase unit against EV. Mean ± SD was shown for three independent experiments. *P* values were calculated with Student's *T*-test.

NIH-PA Author Manuscript
NIH-PA Author Manuscript
NIH-PA Author Manuscript

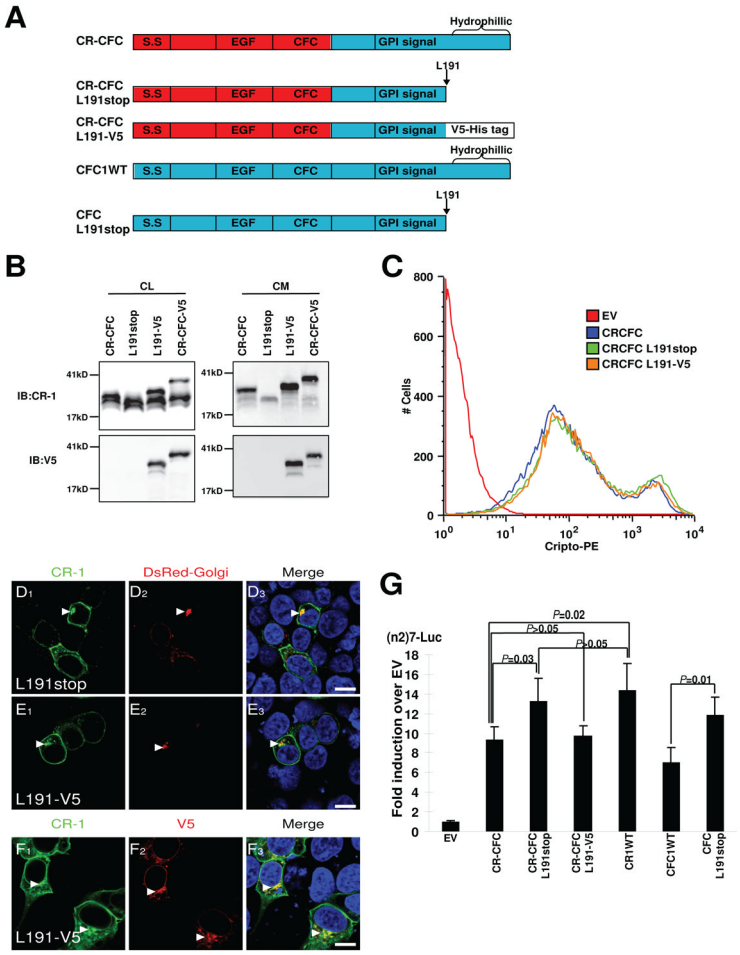

Fig. 9. Biological significance of the COOH-terminal hydrophilic extension of hCFC1 in Nodal signaling

(**A**) Schematic of COOH-terminally deleted CR-CFC or CFC1 construct. Sequences from hCR-1 are shown in red and from hCFC1 in blue. (**B**) Expression of each CR-CFC variant in cell lysates and conditioned medium. 293T cells were transiently transfected with indicated expression vectors. Total cell lysates (CL) and conditioned medium (CM) were collected 24 h after transfection. Immunoblot analysis was performed with the anti-hCR-1 antibody (upper panel) and the same blots were then stripped and reblotted with the anti-V5 antibody (lower panel). (**C**) FACS analysis of cell-surface expression for each CR-CFC variant. 293T cells transiently transfected with the indicated expression vectors were stained with PE-conjugated anti-hCR-1 mAb and analyzed with FACS. EV was used as a negative control. (**D–F**) Immunocytochemical analysis of each CR-CFC variant in transiently transfected 293T cells after permeabilization. CR-1 proteins were stained with anti-CR-1 mAb (**D_1–E_1**) (green). DsRed-Golgi was co-transfected with each CR-CFC construct in **D_2–E_2** (red). Co-staining of CR-CFC L191-V5 with anti-CR-1 mAb (**F_1**, green) and anti-V5 antibody (**F_2**, red) is shown in **F**. Nuclei were counterstained with DAPI (blue) and tricolor merged images are shown in **D_3–F_3**. Images were visualized by confocal microscopy. Arrowheads indicate Golgi localization of the CR-CFC protein. Scale bar = 10 μm. (**G**) (n2)7-Luc reporter assay. Serum starved 293T cells were transiently transfected with the (n2)7-Luc reporter, TK renilla reporter, mFast-1, mNodal-V5, ALK4-HA expression vector and the indicated expression vectors. Values indicate fold induction of relative luciferase unit against EV.

Mean ± SD was shown for three independent experiments. *P* values were calculated with Student's *T*-test.

NIH-PA Author Manuscript
NIH-PA Author Manuscript
NIH-PA Author Manuscript